On the investigation of composite cooling/heating set gel systems based on rice starch and curdlan

Jing Wang[1], Qianhui Ma[1], Pingxiong Cai[2], Xinyu Sun[1], Qingjie Sun[1,3], Man Li[1,3,*], Yanfei Wang[1,3,†], Lei, Zhong[4], Fengwei Xie[5]

[1]*College of Food Science and Engineering, Qingdao Agricultural University, Qingdao, Shandong 266109, China*

[2]*Guangxi Key Laboratory of Green Chemical Materials and Safety Technology, Guangxi Engineering Research Center for New Chemical Materials and Safety Technology, Beibu Gulf University, Qinzhou, Guangxi 535000, China*

[3]*Qingdao Special Food Research Institute, Qingdao, Shandong 266109, China*

[4]*Guangxi Key Laboratory for Polysaccharide Materials and Modifications, Guangxi Higher Education Institutes Key Laboratory for New Chemical and Biological Transformation Process Technology, School of Chemistry and Chemical Engineering, Guangxi Minzu University, Nanning, Guangxi 530006, China*

[5]*School of Engineering, Newcastle University, Newcastle upon Tyne, NE1 7RU, United Kingdom*

[*]Corresponding author. *E-mail address*: manliqau@163.com (M. Li),

[†]Corresponding author. *E-mail addresses*: yanfeiwang@qau.edu.cn; yanfeiwangqau@163.com (Y. Wang)

Abstract

In pursuit of advancing the understanding of composite gel systems, this study delves into the intricate realm of rheology, structural elucidation, and mechanical attributes. Specifically, it scrutinizes the symbiotic interplay between rice starch, a cooling-set gel, and curdlan, a thermo-irreversible heating-set gel. A higher curdlan content enhances the inter-chain hydrogen bonding between rice starch and curdlan, resulting in a denser gel structure and thus increased moduli, solid-like behavior, and mechanical properties, and reduced frequency-dependence, especially at high temperatures (>65 °C). For example, with 50% curdlan incorporation, G' (90 °C) improved by 252%. Notably, thermal treatment can compromise the structural integrity of the rice starch gel, reducing strength and softening texture. However, this textural degradation can be effectively mitigated with, for example, 30% curdlan incorporation, resulting in a 55-fold hardness increase at 85 °C. The knowledge gained from this work offers valuable guidance for tailoring starch-based gel products to specific properties.

Keywords: rice starch; curdlan; rheological properties; fractal structure; textural properties; composite gels

1 Introduction

Fresh rice products, such as rice noodles and rice cakes, are beloved staples foods in many Asian countries and are enjoyed worldwide for their delightful taste and tender texture (Cao, Zhao, Jin, Tian, Zhou, & Long, 2021; C. Li, You, Chen, Gu, Zhang, Holler, et al., 2021). However, these high-moisture, nutrient-rich foods are susceptible to microbial deterioration at room temperature, resulting in a short shelf life (Kang, Han, Lee, Ryu, Kim, Cho, et al., 2022). Thermal treatment, which deactivates microorganisms by disrupting the cell membranes, ribosomes, and nucleic acids, is considered an effective food preservation technique and plays an important role in the food industry (Khan, Tango, Miskeen, Lee, & Oh, 2017).

Rice starch (RS), as the major component of the rice grain, plays a crucial role in shaping the specific structural network and quality of rice-based products (C. Li, et al., 2021). When heated in water, starch undergoes gelatinization, then forming a stable, interconnected three-dimensional network structure after cooling (Cui, Jia, Sun, Yu, Ji, Dai, et al., 2022). However, RS gels tend to be fragile, especially when subjected to thermal treatment that disrupts hydrogen bonds and damages the structural network of the gels, resulting in rice products with a delicate texture (Auksornsri, Bornhorst, Tang, Tang, & Songsermpong, 2018).

Many studies have been carried out to improve the quality of rice products. As common food additives and suitable natural colloids in the food industry, various polysaccharides (e.g. locust bean gum, xanthan gum, hydroxypropyl methylcellulose, and β-glucan) and proteins (e.g. soybean protein, egg-albumin, and rice protein) have been used to improve the quality of RS gel foods (C. Li, et al., 2021; Low, Effarizah, & Cheng, 2020; Satrapai & Suphantharika, 2007; Villanueva, De Lamo, Harasym, & Ronda, 2018). Although the aforementioned food additives have been able to improve the quality of rice products to some extent, the problems of soft and brittle texture have yet to be fully addressed.

Curdlan (CD), a type of 1,3-β-D-glucan, is an FDA-approved food additive. It serves as a

versatile stabilizer, thickener and texturizer in the food industry, readily incorporated as needed during food production (Verma, Niamah, Patel, Thakur, Sandhu, Chavez-Gonzalez, et al., 2020). CD has recently attracted considerable attention due to its unique thermo-irreversible heat-set property, which means gelation occurs at temperatures above 80 °C (Y. Chen & Wang, 2020; Klimek, Przekora, Benko, Niemiec, Blazewicz, & Ginalska, 2017). In previous studies, CD was successfully used to improve gel properties, especially in noodles (T. Chen, Fang, Zuo, & Liu, 2016; Han, Seo, Lim, & June, 2011; Kuang, Yang, Huang, Cao, Pu, Ma, et al., 2022). However, there is limited knowledge of the interaction mechanism between RS and CD, which restricts its widespread application in rice products.

In this study, RS-CD composite gels with different RS/CD ratios (10:0, 7:3, 5:5, 3:7, and 0:10) were prepared. Our hypothesis is that CD, as a thermo-irreversible heating-set gel, has the capacity to create a gel network during starch gelatinization and an interspersed dual network structure with the RS gel when cooling occurs, thereby enhancing the mechanical properties of the gel. In contrast, most previous studies have primarily focused on the effect of a small amount of curdlan (<10%) on the pasting and rheological properties of starch (T. Chen, Fang, Zuo, & Liu, 2016) or the cooking characteristics and textural properties of starchy gel-based foods (Han, Seo, Lim, & June, 2011). The main objective of this study was to carry out a comprehensive examination of the interactions between RS and CD, utilizing RS-CD as a model to unravel the structure-property relationships in composite cooling/heat-set-gel systems. The insights derived from this research have the potential to steer the development of high-quality RS gel-based foods.

2 Materials and method

2.1 Materials

A food-grade rice starch (containing 0.88% protein, 0.11% fat, and 0.22% ash) was purchased from Wuxi Jinnong Biotechnology Co., Ltd (Yichun, China). Curdlan (purity 87.6%) was supplied

by Shandong Qidi Food Technology Co., Ltd (Heze, China). All other reagents and chemicals were of analytical purity.

2.2 Sample Preparation

For rheological measurements, RS was mixed with CD as a dry powder and then dispersed in water (25 °C) with stirring for 2 h. The ratios of RS to CD were 10:0, 7:3, 5:5, 3:7, and 0:10 (w/w), and the total biopolymer concentration in water was 5%. To gelatinize the RS, the suspensions were then heated to 95 °C in a water bath and maintained for 1.5 h. The composite solutions were then cooled to 50 °C and transferred to a sealed bottle.

For textural tests, 8% of the desired amount of RS was mixed with water at a ratio of 1:5 (w/w), followed by continuous stirring in a boiling water bath for 1 min to obtain a starch paste. The remaining polymers and water were then added to the starch paste to produce RS-CD composites (5% w/w). For the pure CD sample, the CD powder was dispersed in water with stirring for 2 min. All composites with different RS/CD ratios were placed in a refrigerator at 4 °C for 12 h after steaming for 30 min to obtain composite gels. The composite gels were brought to room temperature before testing at 25 °C. These composite gels were heated at 85 °C for half an hour before testing at 85 °C.

2.3 Rheological measurements

Dynamic rheological tests were performed using a strain-controlled rheometer (MCR302, Anton Paar, Austria) equipped with a parallel-plate geometry system (50 mm diameter and 1 mm gap).

Strain sweeps were performed in the range of 0.01–1000% at a frequency of 1 Hz at 25 °C to obtain the linear range of viscoelasticity.

Temperature sweeps were carried out from 25 °C to 95 °C. The heating rate was set to 2 °C/min and the frequency at 1 Hz. The sample was filled in the gap between the plates, and then corn germ oil was applied to prevent liquid evaporation.

Frequency sweeps from 0.1 rad/s to 100 rad/s were conducted at 25 °C and 85 °C. The frequency-dependence of storage modulus (G') and loss modulus (G'') can be shown in Eqs. (1) and (2).

$$G' = G_0'\omega^{n'} \quad (1)$$

$$G'' = G_0''\omega^{n''} \quad (2)$$

Here, G' (Pa) and G'' (Pa) are the storage modulus and loss modulus, respectively; ω (rad/s) is the angular frequency; n' and n'' are the slopes of log G' *vs.* log ω and log G'' *vs.* log ω, respectively; G_0' (Pa) and G_0'' (Pa) are the intercepts of log G' *vs.* log ω and log G'' *vs.* log ω, respectively, and n is a constant (Ortega-Ojeda, Larsson, & Eliasson, 2004). The calculated results are shown in Table S1.

2.4 Small-angle X-ray scattering (SAXS)

SAXS analysis of the gels was conducted using a SAXS facility (Nano-inXider, Xenocs, France). The gel sample was placed on the sample rack and measured for 5 min. With air as the background, the XSACT analysis software was used to acquire the 1D curves from 2D images, and the data within the angular range of $0.003 < q < 0.368$ Å^{-1} were collected as SAXS patterns, where $q = 4\pi\sin\theta/\lambda$, with 2θ representing the scattering angle and λ denoting the X-ray wavelength of the X-ray source. Before further analysis, all data were normalized and had background subtraction performed. The moisture contents of all samples are listed in Table S2.

2.5 Scanning Electron Microscopy (SEM)

An SEM system (JSM-7500F, Japan Electronic Instruments Co., Ltd., Japan) with an accelerating voltage of 10 kV was used to observe the fracture surface of the samples. The samples were first frozen in liquid nitrogen and then freeze-dried for 24 h. Before observation, the samples

were sputter-coated with gold and fixed on copper stubs. Images were collected at 500 × and 1000 × magnifications.

2.6 Fourier transform infrared spectroscopy (FTIR)

A spectrometer (Nicolet iS10, Thermo, America) was used to obtain FTIR spectra for RS-CD gels. Tests were conducted in the range of 500–4000 cm^{-1} with a resolution of 4 cm^{-1} and 64 scans.

2.7 Differential scanning calorimetry (DSC)

A DSC system (DSC-1, Mettler Toledo, Switzerland) equipped with a recirculated cooling system (METT FT900) was utilized to investigate the thermal properties of RS-CD gels. Before testing, instrument calibration was performed using indium and zinc. The sample weighing 5–10 mg was carefully placed in a DSC aluminum pan and hermetically sealed. Temperature ramping from −40 °C to 140 °C occurred at a rate of 10 °C/min (Cheng, Zhang, Qiao, Yan, Zhao, Jia, et al., 2022). Ultra-pure nitrogen gas with a flow rate of 50 mL/min was applied as the protective gas. An empty aluminum pan was used as the control. Test results were computed using STARe software (Mettler Toledo, Switzerland).

2.8 Texture profile analysis (TPA)

A texture analyzer (TA.XT PlusC, Stable Micro Systems Ltd, UK) was used to investigate the textural characteristics of RS-CD gels. The TPA model was used to compress the samples using a P/36R probe, a test speed of 1.0 mm/s, a strain of 30%, and a trigger force of 5 g. All tests were performed at least three times.

2.9 Statistical Analysis

Each sample underwent a minimum of three parallel tests, and the data were presented as the mean ± standard deviation. Variance analysis was performed using SPSS 16.0 software, and means

were compared using the Duncan test. A significance level $p<0.05$ was deemed statistically significant.

3 Results and Discussions

3.1 Rheological properties of RS-CD composites

3.1.1 Linear viscoelastic regions

Dynamic measurements generally have been used to understand the evolution of the internal structure of, and molecular interactions in, the samples during the network formation (Musampa, Alves, & Maia, 2007). The *G′* of hydrogels is determined by the hardness, the strength of the junction zone, and the binding amount of the effective molecular chains, while the frictional energy consumption in the liquid state, which involves the vibration and rotation of functional groups, the motion and friction of small molecules, and the mobility, contributes to *G″* (Y. Wang, Yu, Xie, Li, Sun, Liu, et al., 2018). Therefore, the gelation behavior and structural characteristics of RS-CD composite gels can be detected by *G′* and *G″*.

Fig. S1 shows the strain sweep curves for RS-CD composite samples performed over a strain range of 0.01–1000%. It can be seen that, with increasing strain, *G′* remained constant, i.e. in the linear viscoelastic region, followed by a sharp decrease. At a lower strain, all the samples showed a solid-like gel state ($G' > G''$). With increasing strain, there was a crossover point of *G′* and *G″*, indicating a textural transition from solid to liquid. The crossover points for the pure RS and CD samples were observed at around 250% strain and 15% strain, respectively. However, the moduli of pure CD were higher than those of pure RS in the linear viscoelastic region. This suggests that although pure CD was a stronger gel than pure RS, the former was destroyed more quickly. The linear viscoelastic region of pure RS was the widest, and that of the composite samples gradually narrowed as the proportion of CD increased. When the strain for pure CD was higher than 0.6%, *G′*

showed a significant downward trend. Therefore, in the following dynamic rheological tests, the strain was set at 0.1%.

3.1.2 Gelation behavior of RS-CD composites during heating

Fig. 1 shows G', G'', and tan δ *vs.* temperature curves for RS-CD composites. For all samples, G'' was always lower than G' throughout the testing temperature range, suggesting a solid-like behavior contributed by chain interactions. For pure RS, G' and G'' reduced with increasing temperature attributed to the rupture of inter-chain hydrogen bonding between RS during thermal processing (Borchers & Pieler, 2010). In addition, the G' of RS was less than 100 Pa, indicating a weak gel property of pure RS (G. Li, Huang, Deng, Guo, Cai, Zhang, et al., 2022).

For pure CD, G' first showed a decrease and then an increase with increasing temperature, and G'' presented a similar pattern of change except for a peak occurring between about 48 °C to 70 °C. The reduction in G' at the initial heating stage may be due to the partial destruction of hydrogen bonds between CD chains and the subsequent release of CD microfibers from fiber bundles, resulting in a reduced CD gel strength (Xiao, Jiang, Wu, Yang, Ni, Yan, et al., 2017). At higher temperatures, G' increased gradually with increasing temperature attributed to the hydrophobic association of the released microfibers and the formation of a stable gel network structure (Konno & Harada, 1991). In the temperature range of 48–70 °C, both effects were present and competed with each other.

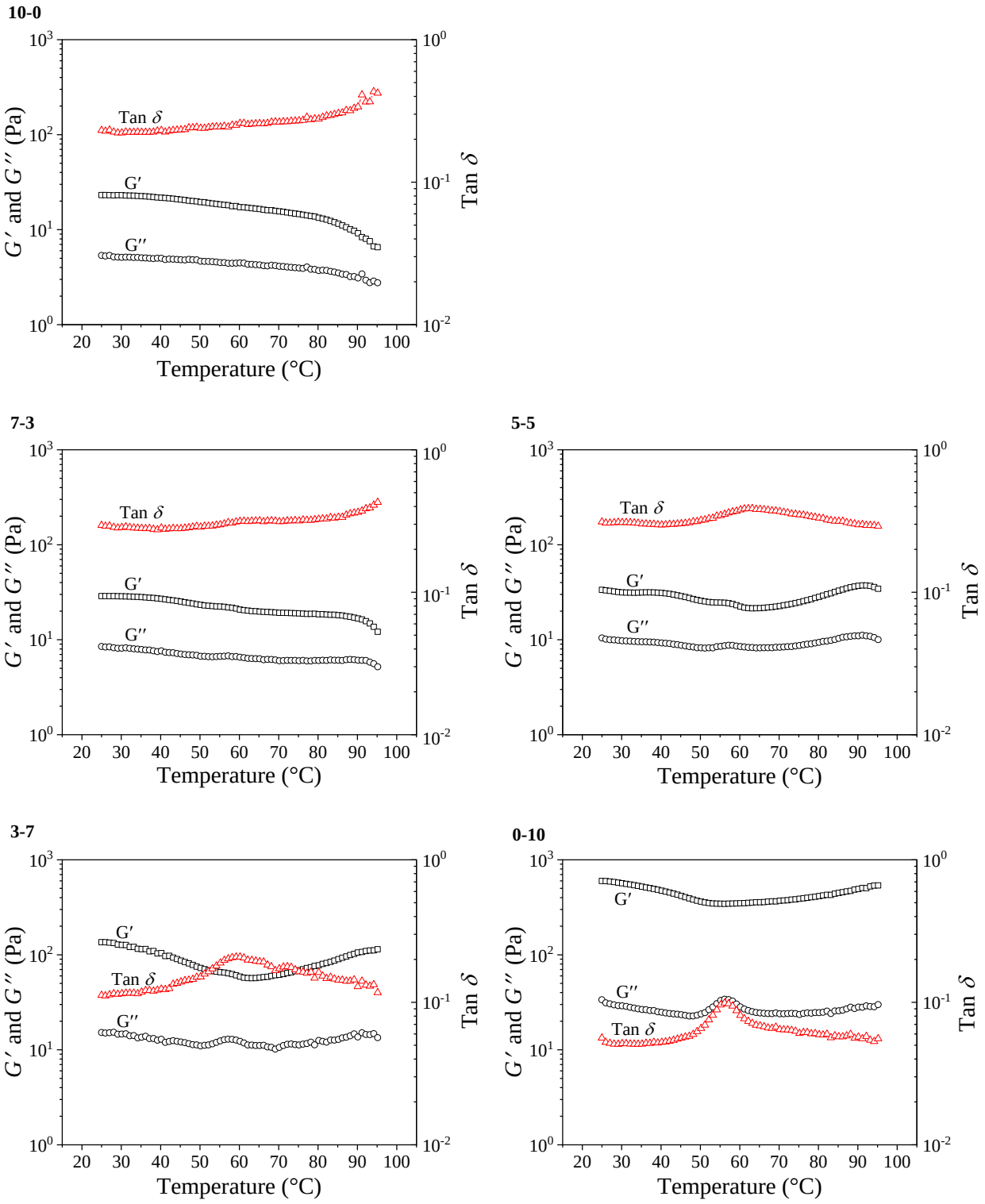

Fig. 1. *G′*, *G″* and tan *δ* curves for RS-CD composite gels (10:0, 7:3, 5:5, 3:7, and 0:10) in temperature scanning mode.

For the composite samples, the temperature-scanning curves showed two different trends, which are roughly parallel to those for pure RS and CD. The temperature-scanning profiles for the RS-CD composite containing 70% RS showed a similar trend to that for pure RS, suggesting that RS dominated in structure formation. In contrast, composites with low RS content (≤50%) showed similar temperature-scanning curves to pure CD, suggesting the dominant role of CD in the gel behavior. In addition, with increasing RS content, the turning point of G' and the peak of tan δ were shifted to higher temperatures, and the peak value of G'' reduced. This implies that the incorporation of RS reduced the thermal gelling ability of CD and shortened the competitive process of hydrogen-bond cleavage and hydrophobic association. Compared with pure starch gel, the gel strength of composite gels at high temperatures was improved, and the decrease in modulus with increasing temperature for composite gels was reduced. These behaviors may be attributed to the thermo-irreversible heat-set gel property of CD, which can form a compact gel structure at high temperatures. It can be confirmed by the results of fractal structure analysis.

RS-CD composites had moduli intermediate between those of individual RS and CD. Moreover, both G' and G'' were increased with a higher proportion of CD, suggesting that the incorporation of CD formed a stronger gel structure. In particular, the G' of composite gels at high temperatures (>65 °C) increased sharply with increasing CD content. For example, compared to pure RS, the G' at 30 °C for the 7:3, 5:5, and 3:7 RS-CD composite samples was increased by 17%, 34%, and 428%, respectively, and the G' at 90 °C for the 7:3, 5:5, and 3:7 RS-CD composite samples was increased by 80%, 252%, and 1030%, respectively (refer to Table S3).

3.1.3 Dynamic mechanical properties

Fig. S2 shows the G' and G'' data for RS-CD composite samples under frequency sweeps at 25 °C. All the samples show a typical solid-like behavior ($G' > G''$) (Qiao, Luo, Li, Jiang, & Zhang, 2023). Generally, a higher frequency resulted in a higher G' than G'', suggesting that the material was more solid-like. The n', n'', G_0' and G_0'' values for RS-CD composite gels at 25 °C were listed in

Table S1. For all the samples, n' was much lower than n'', and G' was less dependent on frequency than G'', indicating that these samples were less viscous and more elastic (Park, Chung, & Yoo, 2004; Y. Wang, et al., 2018).

For the pure samples, both G' and G'' of RS are lower than that of CD, indicating better gel properties of CD at room temperature. For the pure CD sample, the value of n' tends to be 0, and G_0'' was much lower than G_0', indicative of a clearly solid-like behavior (Ortega-Ojeda, Larsson, & Eliasson, 2004). Pure RS showed the most apparent frequency-dependence among all the samples due to the highest value of both n' and n''.

For all the composite samples, the moduli (G' and G'') were between those of pure RS and CD, and increased with increasing CD content. With increasing CD content, both n' and n'' decreased, and both G_0' and G_0'' increased, suggesting that the incorporation of CD increased the solid-like behavior of RS.

3.2 Fractal structure

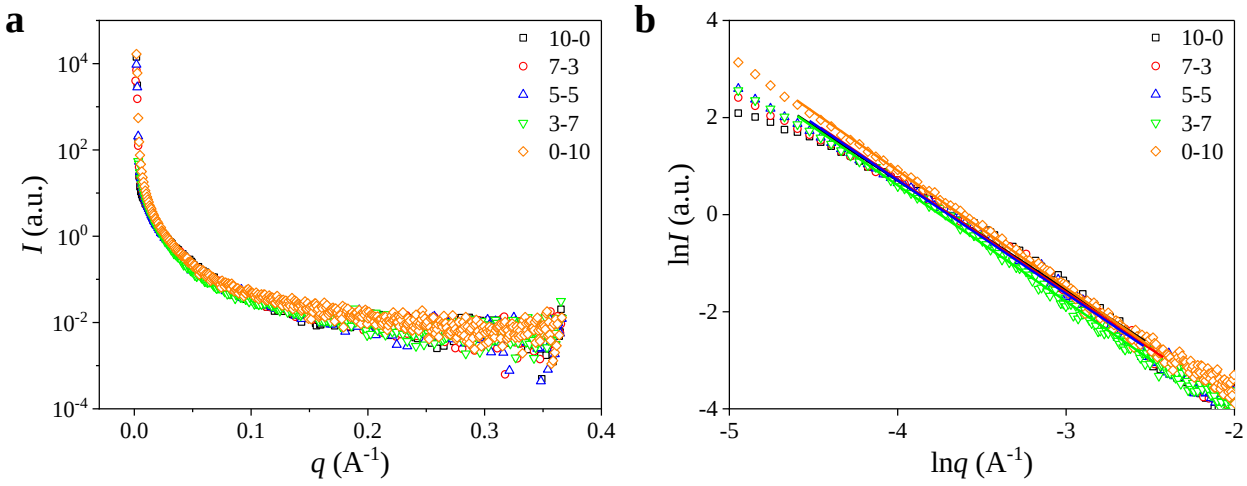

Fig. 2. SAXS intensity profiles (a) and ln$I$ *vs.* ln$q$ curves with their fitted lines (b) for RS-CD composite gels (10:0, 7:3, 5:5, 3:7, and 0:10).

Fig. 2a shows the SAXS intensity profiles for RS-CD composite gels. For all the samples, the scattering intensity in the small-angle range decreased significantly with increasing q, indicating the

formation of a larger-scale network or a greater degree of intermolecular aggregation (Tomsic, Prossnigg, & Glatter, 2008).

To investigate the structural differences among RS-CD composite gels with different ratios, the fractal structure was analyzed according to the Porod equation: $I \propto q^{-\alpha}$, where I and q are the SAXS intensity and scattering vector, respectively, and α is an exponent. For all the samples, a self-similar fractal structure within a certain limit was presented (Fig. 2b), and the Porod slopes (α) were less than 3 (Table S4), suggesting that the RS-CD composite gels had a smooth surface with mass fractal dimension ($D = \alpha$) (Zhang, Jia, Ma, Sun, Li, & Xie, 2024). The D value for pure CD was higher than that for pure RS, indicating that CD formed a more compact gel structure than RS. For composite gels, as the CD content increased, the D value increased, suggesting that the incorporation of CD resulted in a more compact gel.

3.3 Microscopic morphology

Fig. 3 shows the morphological characteristics of the RS-CD composite gels. For the pure RS sample, a honeycomb-like, porous structure with small voids and relatively thin ‘cell walls’ was observed, which may be due to the dehydration and condensation of gelatinized RS molecules during cooling and the eventual formation of a dense aggregation structure (Ren, Rong, Shen, Liu, Xiao, Luo, et al., 2020). Compared with the pure RS gel, the pure CD sample showed a porous structure with larger voids and disrupted ‘cell walls’.

265

RS-CD	500x	1000x
10:0	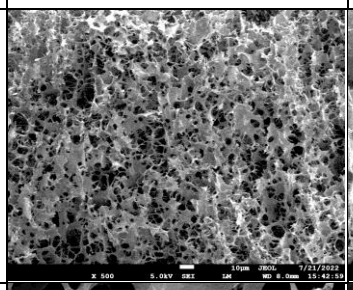	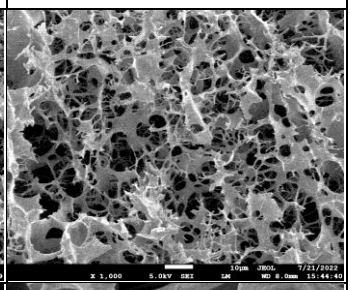
7:3	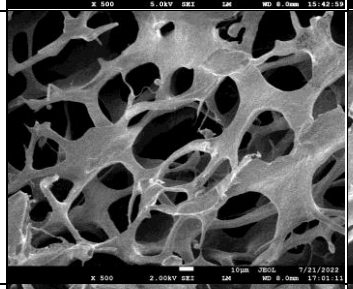	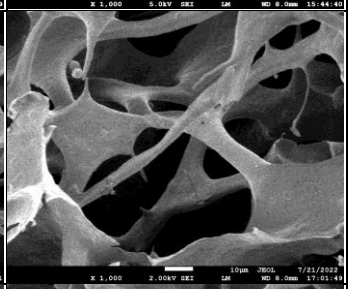
5:5	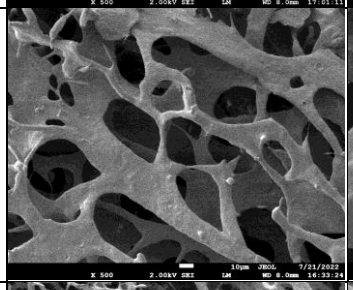	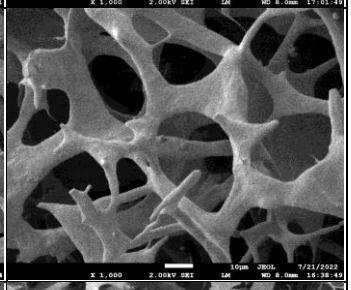
3:7	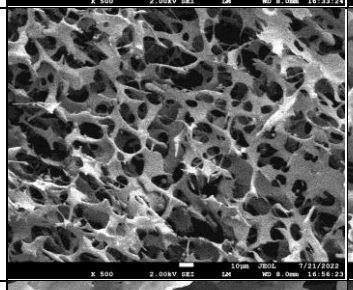	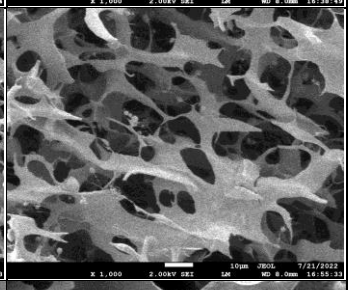
0:10	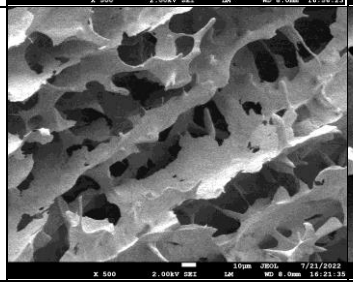	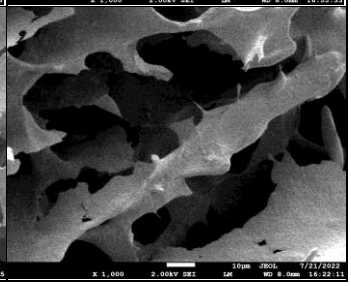

266 **Fig. 3.** SEM images of RS-CD composite gels (10:0, 7:3, 5:5, 3:7, and 0:10) at 500 × and 1000 ×.

267

All the RS-CD composite gels exhibited a honeycomb-like, porous structure with larger voids and stronger ‘cell walls’ compared with the pure RS gel, indicating that the added CD did not simply act as a filler in RS, but rather interspersed into the three-dimensional structure of RS and its interactions with RS molecules enlarged the network gel structure. This confirms our hypothesis that CD can form an interspersed dual network structure with RS. Generally, smaller void sizes and stronger ‘cell walls’ mean a more compact and dense gel structure. A similar phenomenon was noticed in a composite gel system of carrageenan and gelatin (Cheng, et al., 2022). In RS-CD composite gels, as the CD content increased, the size of the voids notably decreased, while the thickness of the ‘cell walls’ exhibited a tendency to increase until a CD content exceeded 50%, after which it decreased. Furthermore, images of the RS-CD composite gels containing 70% CD started revealing disrupted ‘cell walls’. The compactness of RS-CD composite gels is influenced by a delicate balance between void size and ‘cell wall’ thickness.

3.4 FTIR analysis

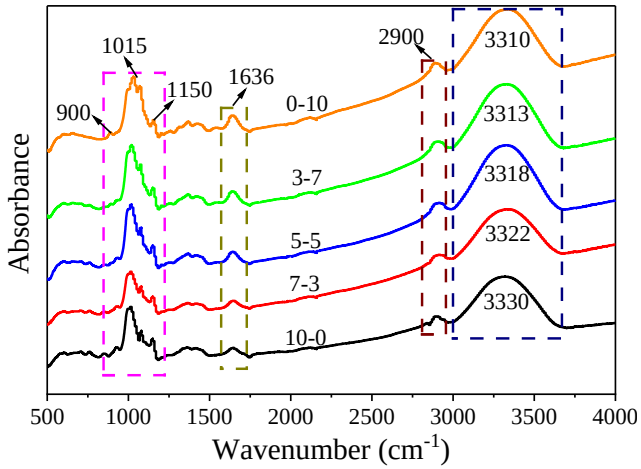

Fig. 4. FTIR spectra of RS-CD composite gels (10:0, 7:3, 5:5, 3:7, and 0:10).

Fig. 4 displays the FTIR spectra for RS-CD composite gels. It can be seen that the infrared spectra for all RS-CD composite samples showed a similar pattern with no new absorption peaks,

suggesting no significant chemical structure changes and covalent bonding during RS-CD composite preparation.

All samples exhibited pronounced fingerprint peaks at about 900 cm^{-1}, 1015 cm^{-1}, and 1150 cm^{-1}, corresponding to β-glycosidic bonds, the stretching vibration of the C-O bond, and the C-O-C bond of polysaccharide molecules, respectively (Klimek, Przekora, Benko, Niemiec, Blazewicz, & Ginalska, 2017; Zhou, Fu, Bian, Chang, & Zhang, 2022). The peak at about 1636 cm^{-1} can be related to associated water (Tao, Guo, Qin, Yu, Wang, Li, et al., 2022). The absorption peak at about 2900 cm^{-1} is considered due to the stretching of C-H (CH_2) groups (Tao, et al., 2022). The peak at about 3300 cm^{-1} can be attributed to hydrogen bonding (Luo, Chen, He, Li, Jia, Hossen, et al., 2022).

In general, the absorption peak of the free -OH group is at about 3600 cm^{-1}, and shifts to a lower wavenumber (red shift) when being involved in hydrogen bonding (Elizondo, Sobral, & Menegalli, 2009). Moreover, the stronger the hydrogen bond formed, the lower is the wave number for this characteristic peak (S. Wang, Ren, Li, Sun, & Liu, 2014). With increasing CD content, the absorption peak for -OH in the composite samples (3330, 3320, 3318, 3313, and 3310 cm^{-1} for the 10:0, 7:3, 5:5, 3:7, and 0:10 RS-CD samples, respectively) gradually shifted to a lower wavenumber, implying that the incorporation of CD could enhance the intra-molecular and inter-molecular hydrogen bonding in the gels (Cui, Li, Ji, Qin, Shi, Qiao, et al., 2022).

3.5 Thermal analysis

Fig. S3 shows the DSC curves for RS-CD composites with different ratios. For all the samples, the heat flow curve exhibited an exothermic peak. For samples with CD content below 50%, the thermal denaturation peak was shifted to higher temperatures with increasing CD content, indicating a stronger interaction between RS and CD, which requires much more energy to break during heating. In particular, the peak temperature for the sample with the 5:5 RS-CD sample was higher than that for pure RS and pure CD, indicating a strong interaction between RS and CD occurring in the composites.

311 The enthalpy change values of the RS-CD composite gels were calculated and presented in
312 Table S5. The enthalpy change value for the pure RS gel was lower than that for the pure CD gel;
313 therefore, the incorporation of CD should lead to a larger peak area. It was observed that increasing
314 the CD content led to an increase in the peak area (enthalpy change), indicating that the RS-CD
315 composite gels are more difficult to unzip from a highly ordered chain (Cheng, et al., 2022).

316 ### 3.6 Textural characteristics

317 Textural characteristics, including hardness, springiness, cohesiveness, gumminess, and
318 chewiness, can systematically reflect the properties of polysaccharide hydrocolloids, which include
319 palatability, mouthfeel and swallowability (Sarkar, Soltanahmadi, Chen, & Stokes, 2021; Yuan, Xu,
320 Cui, & Wang, 2019). Fig. 5 shows the textural characteristics of RS-CD composite gels at 25 °C and
321 85 °C.

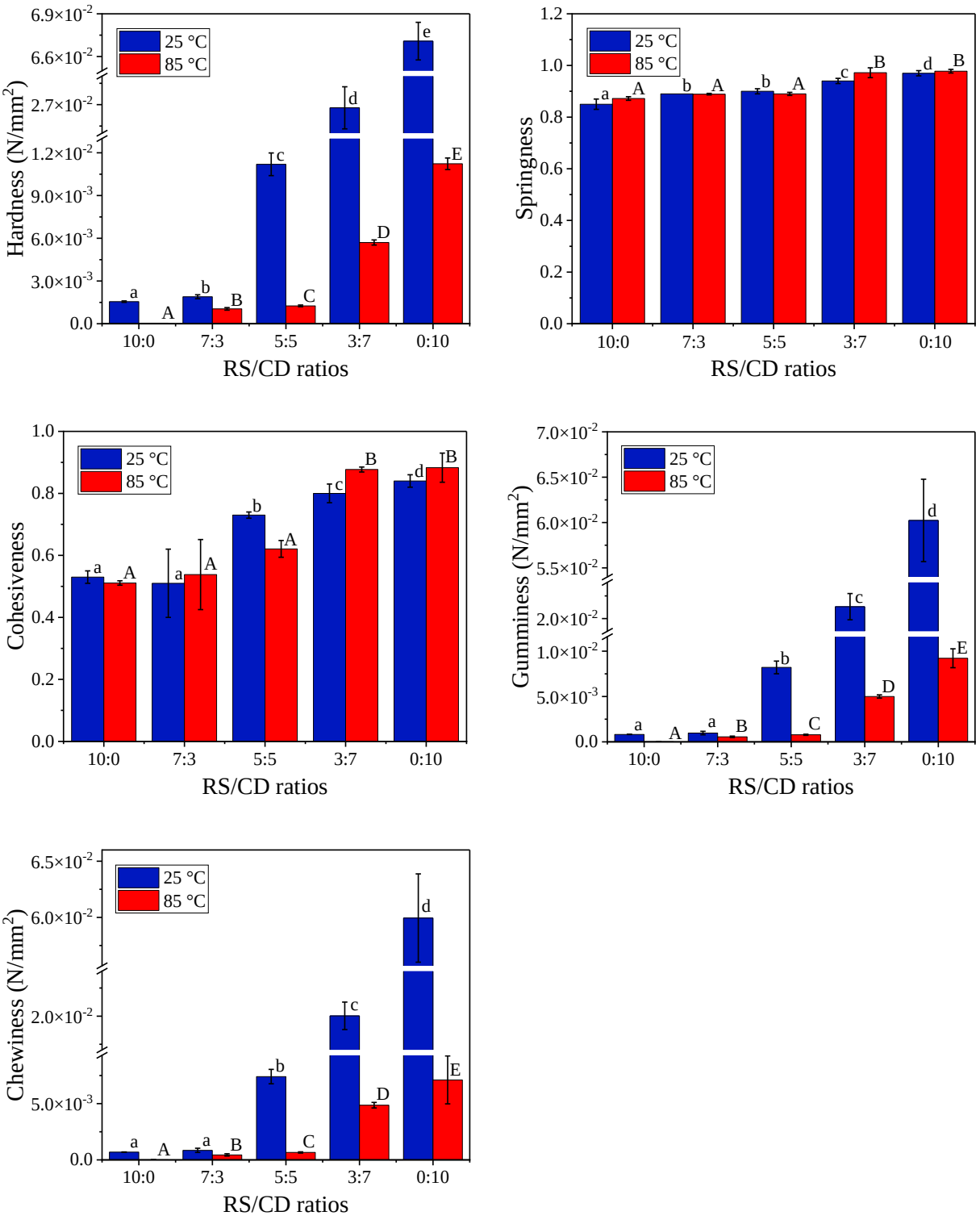

Fig. 5. Textural properties of RS-CD composite gels (10:0, 7:3, 5:5, 3:7, and 0:10) at 25 °C and 85 °C. Within one group (either a, b, c, d, and e, or A, B, C, D and E), different letters mean significant difference at 25 °C and 85 °C ($p < 0.05$).

Hardness, the force required to compress the food between the teeth or between the roof and tongue (Yuan, Xu, Cui, & Wang, 2019), suggests the strength of the hydrogel network (Veiga-Santos, Suzuki, Cereda, & Scamparini, 2005). Springiness, the ability of gels to be compressed and then spring back (Tao, et al., 2022), indicates the elasticity of the gel network. Cohesiveness, the degree of compression between the teeth before a material breaks (Tao, et al., 2022), is related to the internal strength and structural integrity of gels (Min, Ma, Kuang, Huang, & Xiong, 2022). For pure RS, the values of hardness and cohesiveness at 85 °C were lower than those at 25 °C, indicating that the thermal treatment destroyed the structural integrity of the RS gel and led to lower gel strength. This result was consistent with the rheological data of temperature sweep. In addition, there were striking differences in the textural properties between the pure RS gel and the RS-CD composite gels. The incorporation of CD increased the values of hardness, springiness, and cohesiveness of the RS gel at both 25 °C and 85 °C, indicating that a more compact, strong, and elastic gel network was formed. This could be because the CD with a larger number of hydroxyl groups could form inter-chain hydrogen bonds between RS and CD during the composite gel formation, confirmed by the FTIR results, as hydrogen bonding plays an important role in the formation of RS gel (J. Li, Yadav, & Li, 2019).

Gumminess (derived from hardness and cohesiveness) and chewiness (derived from springiness and gumminess) refer to the energy required to burst the gel into a state of being ready to swallow (Yuan, Xu, Cui, & Wang, 2019). It can be seen that, for all samples, both values of gumminess and chewiness at 85 °C were much lower than those at 25 °C, indicating that the high-temperature treatment led to a softer texture. This result aligns with the observation that thermal treatment leads to rice products with a soft and fragile texture (Auksornsri, Bornhorst, Tang, Tang, & Songsermpong, 2018). Compared to the pure RS sample, both the gumminess and chewiness of the composite gel increased with increasing CD content. The results above indicate that the textural deterioration of RS gel due to high temperatures could be mitigated through CD incorporation. For example, compared

to pure RS at 25 °C, the hardness of pure RS at 85 °C exhibited a substantial 98.8% decrease, which is consistent with the observation that thermal treatment leads to rice products with a soft texture (Auksornsri, Bornhorst, Tang, Tang, & Songsermpong, 2018). However, this reduction in hardness was notably diminished to 32.73% and 19.06% with the inclusion of 30% and 50% CD, respectively. Importantly, when integrated with 70% CD, the hardness at 85 °C became much higher than that of pure RS at 25 °C.

3.7 Temperature-induced gelation process of RS-CD composites

According to the classical rheological behavior of polymer solution and gel, combined with the rheological results of RS-CD composites discussed above, we propose a schematic representation of the temperature-induced structural changes of the RS-CD composite system, as shown in Fig. 6.

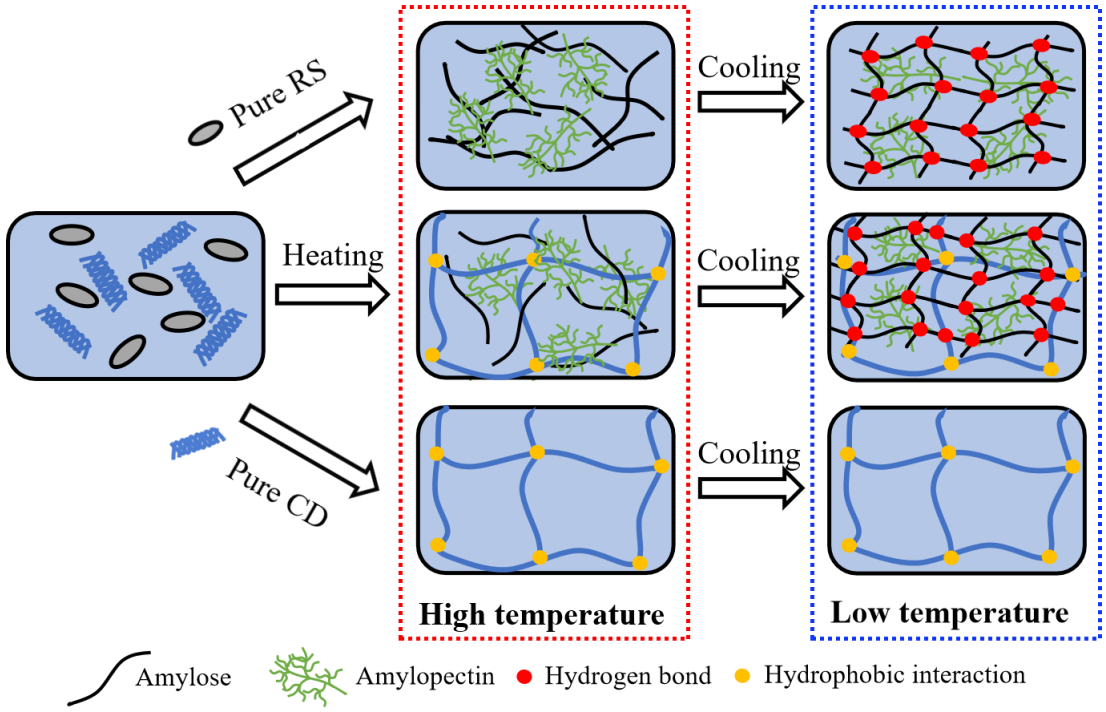

Fig. 6. Schematic representation of temperature-induced structural changes of pure RS, CD and RS-CD composites.

For pure RS, starch granules undergo water absorption, swelling, amylose exudation and granule rupture with excess water and heating, complete starch gelatinization (Cui, Jia, et al., 2022). Therefore, starch molecules in starch paste are present as flexible chains at high temperatures. After cooling, the inter-chain hydrogen bonds between the amylose chains are strengthened, leading to a three-dimensional gel network with embedded amylopectin.

During heating, the triple-stranded helices of CD undergo hydration, swelling, and eventual separation into single helices (Xiao, et al., 2017). At elevated temperatures, the solitary CD chains crosslink through hydrophobic interactions, forming a robust high-set gel network structure. This transition is irreversible and persists as the gel structure after cooling (Y. Chen & Wang, 2020).

In the case of composite samples, the water absorption and swelling of RS granules coincide with the hydration and swelling of the triple-stranded helices of CD in the aqueous solution during heating. As the temperature increases, amylose chains leach out, and RS granules undergo rupture, while the triple-stranded helices of CD completely dissociate. At higher temperatures, CD forms a three-dimensional gel network, with amylose and amylopectin chains embedded in it. Upon cooling, amylose chains establish a secondary network, the RS gel, through hydrogen bonding between the chains. Moreover, hydrophobic interactions among CD molecules, exposing hydroxyl groups in the CD chains, result in inter-chain hydrogen bonding with the RS chains. Therefore, at low temperatures, the RS-CD composite system generates an interpenetrating dual network structure.

4 Conclusion

In this work, novel composite cooling/heating-set-gel systems were prepared, of which the rheological properties, gel structure, mechanical properties, and thermal properties can be significantly influenced by the individual gels (RS and CD) and the interaction between the two.

As a thermo-irreversible heating-set gel, the introduction of CD initiates the primary gel network and eventually forms an interspersed dual network structure with the RS cooling-set gel. The

interaction between the added CD and RS leads to the formation of a denser gel structure, thus enhancing the *G'* and textural properties of the composite gel. FTIR and DSC analyses confirmed the formation of inter-chain hydrogen bonds between CD and RS. The incorporation of CD leads to larger voids and sturdier 'cell walls' within the honeycomb-like porous gel structure. A higher CD content in the composite gel corresponds to increased structural compactness, as reflected by a higher fractal dimension.

Incorporating CD improved the solid-like behavior and gel strength of RS, reducing the frequency-dependent characteristics, especially at elevated temperatures. A higher CD content in the composite gel translates to enhanced mechanical properties, characterized by increased values of hardness, springiness, gumminess, and chewiness. Moreover, with increasing CD content, the dominant influence on rheological properties shifts from RS to CD when the RS ratio reaches 50%. It is worth noting that, for pure RS, being a cooling-set gel, thermal treatment can compromise the structural integrity, leading to lower strength and a softer texture. This textural degradation of RS gel can be significantly ameliorated through CD incorporation.

The work demonstrates the potential for customizing gel structure and properties and elucidates the gelation mechanism of RS-CD hybrid systems. It offers valuable insights for the development of starch-based gel products with enhanced properties.

Acknowledgements

This work was financially supported by the National Natural Science Foundation of China (Grant No. 32302145), the Natural Science Foundation of Shandong Province (Grant No. ZR2021QC192), the Program for Youth Science Innovation in Colleges and Universities in Shandong Province (Grant No. 2020KJF005), the Key R&D Plan of Shandong Province (Grant No. 2022CXGC010604), the Research Fund of Qingdao Special Food Research Institute (Grant No. 66120008), the Cooperation Project with Enterprise (Grant No. 6602422238), the Doctoral Foundation of Qingdao Agricultural

University (Grant No. 6631120081), and the Guangxi Key Laboratory of Green Chemical Materials and Safety Technology, Beibu Gulf University (Grant No. 2022SYSZZ05).

Conflicts of interest

There are no conflicts of interest to declare.

References

Auksornsri, T., Bornhorst, E. R., Tang, J., Tang, Z., & Songsermpong, S. (2018). Developing model food systems with rice based products for microwave assisted thermal sterilization. *Lwt-Food Science and Technology, 96*, 551-559. https://doi.org/10.1016/j.lwt.2018.05.054.

Borchers, A., & Pieler, T. (2010). Programming pluripotent precursor cells derived from Xenopus embryos to generate specific tissues and organs. *Genes (Basel), 1*, 413-426. https://doi.org/10.3390/genes1030413.

Cao, Y., Zhao, J., Jin, Z., Tian, Y., Zhou, X., & Long, J. (2021). Improvement of rice bran modified by extrusion combined with ball milling on the quality of steamed brown rice cake. *Journal of Cereal Science, 99*, 103229. https://doi.org/10.1016/j.jcs.2021.103229.

Chen, T., Fang, S., Zuo, X., & Liu, Y. (2016). Effect of curdlan and xanthan polysaccharides on the pasting, rheological and thermal properties of rice starch. *Journal of Food Science and Technology, 53*, 4076-4083. https://doi.org/10.1007/s13197-016-2414-6.

Chen, Y., & Wang, F. (2020). Review on the preparation, biological activities and applications of curdlan and its derivatives. *European Polymer Journal, 141*, 110096. https://doi.org/10.1016/j.eurpolymj.2020.110096.

Cheng, Z., Zhang, B., Qiao, D., Yan, X., Zhao, S., Jia, C., Niu, M., & Xu, Y. (2022). Addition of κ-carrageenan increases the strength and chewiness of gelatin-based composite gel. *Food Hydrocolloids, 128*, 107565. https://doi.org/10.1016/j.foodhyd.2022.107565.

Cui, C., Jia, Y., Sun, Q., Yu, M., Ji, N., Dai, L., Wang, Y., Qin, Y., Xiong, L., & Sun, Q. (2022). Recent advances in the preparation, characterization, and food application of starch-based hydrogels. *Carbohydrate Polymers, 291*, 119624. https://doi.org/10.1016/j.carbpol.2022.119624.

Cui, C., Li, M., Ji, N., Qin, Y., Shi, R., Qiao, Y., Xiong, L., Dai, L., & Sun, Q. (2022). Calcium alginate/curdlan/corn starch@calcium alginate macrocapsules for slowly digestible and resistant starch. *Carbohydrate Polymers, 285*, 119259. https://doi.org/10.1016/j.carbpol.2022.119259.

Elizondo, N. J., Sobral, P. J. A., & Menegalli, F. C. (2009). Development of films based on blends of Amaranthus cruentus flour and poly(vinyl alcohol). *Carbohydrate Polymers, 75*, 592-598. https://doi.org/10.1016/j.carbpol.2008.08.020.

Han, J.-A., Seo, T.-R., Lim, S.-T., & June, P. D. (2011). Utilization of Rice Starch with Gums in Asian Starch Noodle Preparation as Substitute for Sweet Potato Starch. *Journal of food science and technology, 53*, 4076-4083. https://doi.org/10.1007/s10068-011-0162-y.

Kang, J. H., Han, J.-Y., Lee, H. S., Ryu, S., Kim, S. B., Cho, S., Kang, D.-H., & Min, S. C. (2022). Plasma-activated water effectively decontaminates steamed rice cake. *Lwt-Food Science and Technology, 157*, 112838. https://doi.org/10.1016/j.lwt.2021.112838.

Khan, I., Tango, C. N., Miskeen, S., Lee, B. H., & Oh, D.-H. (2017). Hurdle technology: A novel approach for enhanced food quality and safety – A review. *Food Control, 73*, 1426-1444. http://dx.doi.org/10.1016/j.foodcont.2016.11.010.

Klimek, K., Przekora, A., Benko, A., Niemiec, W., Blazewicz, M., & Ginalska, G. (2017). The use of calcium ions instead of heat treatment for beta-1,3-glucan gelation improves biocompatibility of the beta-1,3-glucan/HA bone scaffold. *Carbohydrate Polymers, 164*, 170-178. http://dx.doi.org/10.1016/j.carbpol.2017.02.015.

Konno, A., & Harada, T. (1991). Thermal properties of curdlan in aqueous suspension and curdlan gel. *Food Hydrocolloids, 5*, 427-434. https://doi.org/10.1016/S0268-005X(09)80101-X.
Kuang, J., Yang, Q., Huang, J., Cao, Y., Pu, H., Ma, W., Min, C., & Xiong, Y. L. (2022). Curdlan-induced rheological, thermal and structural property changes of wheat dough components during heat treatment. *Journal of Cereal Science, 107*, 103528. https://doi.org/10.1007/s13197-016-2414-6.
Li, C., You, Y., Chen, D., Gu, Z., Zhang, Y., Holler, T. P., Ban, X., Hong, Y., Cheng, L., & Li, Z. (2021). A systematic review of rice noodles: Raw material, processing method and quality improvement. *Trends in Food Science & Technology, 107*, 389-400. https://doi.org/10.1016/j.tifs.2020.11.009.
Li, G., Huang, K., Deng, J., Guo, M., Cai, M., Zhang, Y., & Guo, C. F. (2022). Highly Conducting and Stretchable Double-Network Hydrogel for Soft Bioelectronics. *Advanced Materials, 34*(15), 2200261. https://doi.org/10.1002/adma.202200261.
Li, J., Yadav, M. P., & Li, J. (2019). Effect of different hydrocolloids on gluten proteins, starch and dough microstructure. *Journal of Cereal Science, 87*, 85-90. https://doi.org/10.1016/j.jcs.2019.03.004.
Low, Y. K., Effarizah, M. E., & Cheng, L. H. (2020). Factors Influencing Rice Noodles Qualities. *Food Reviews International, 23*, 781-794. https://doi.org/10.1080/87559129.2019.1683747.
Luo, S., Chen, J., He, J., Li, H., Jia, Q., Hossen, M. A., Dai, J., Qin, W., & Liu, Y. (2022). Preparation of corn starch/rock bean protein edible film loaded with d-limonene particles and their application in glutinous rice cake preservation. *International Journal of Biological Macromolecules, 206*, 313-324. https://doi.org/10.1016/j.ijbiomac.2022.02.139.
Min, C., Ma, W., Kuang, J., Huang, J., & Xiong, Y. L. (2022). Textural properties, microstructure and digestibility of mungbean starch–flaxseed protein composite gels. *Food Hydrocolloids, 126*, 107482. https://doi.org/10.1016/j.foodhyd.2022.107482.
Musampa, R. M., Alves, M. M., & Maia, J. M. (2007). Phase separation, rheology and microstructure of pea protein–kappa-carrageenan mixtures. *Food Hydrocolloids, 21*, 92-99. https://doi.org/10.1016/j.foodhyd.2006.02.005.
Ortega-Ojeda, F. E., Larsson, H., & Eliasson, A.-C. (2004). Gel formation in mixtures of amylose and high amylopectin potato starch. *Carbohydrate Polymers, 57*, 55-66. https://doi.org/10.1016/j.carbpol.2004.03.024.
Park, S., Chung, M.-G., & Yoo, B. (2004). Effect of Octenylsuccinylation on Rheological Properties of Corn Starch Pastes. *Starch - Stärke, 56*, 399-406. https://doi.org/10.1002/star.200300274.
Qiao, D., Luo, M., Li, Y. S., Jiang, F. T., & Zhang, B. J. (2023). New evidence on synergistic binding effect of konjac glucomannan and xanthan with high pyruvate group content by atomic force microscopy. *Food Hydrocolloids, 136*, 108232. https://doi.org/10.1016/j.foodhyd.2022.108232.
Ren, Y., Rong, L., Shen, M., Liu, W., Xiao, W., Luo, Y., & Xie, J. (2020). Interaction between rice starch and Mesona chinensis Benth polysaccharide gels: Pasting and gelling properties. *Carbohydrate Polymers, 240*, 116316. https://doi.org/10.1016/j.carbpol.2020.116316.
Sarkar, A., Soltanahmadi, S., Chen, J., & Stokes, J. R. (2021). Oral tribology: Providing insight into oral processing of food colloids. *Food Hydrocolloids, 117*, 106635. https://doi.org/10.1016/j.foodhyd.2021.106635.
Satrapai, S., & Suphantharika, M. (2007). Influence of spent brewer's yeast β-glucan on gelatinization and retrogradation of rice starch. *Carbohydrate Polymers, 67*, 500-510. https://doi.org/10.1016/j.carbpol.2006.06.028.
Tao, H., Guo, L., Qin, Z., Yu, B., Wang, Y., Li, J., Wang, Z., Shao, X., Dou, G., & Cui, B. (2022). Textural characteristics of mixed gels improved by structural recombination and the formation of hydrogen bonds between curdlan and carrageenan. *Food Hydrocolloids, 129*, 107678. https://doi.org/10.1016/j.foodhyd.2022.107678.
Tomsic, M., Prossnigg, F., & Glatter, O. (2008). A thermoreversible double gel: characterization of a methylcellulose and kappa-carrageenan mixed system in water by SAXS, DSC and rheology. *Journal of Colloid and Interface Science, 322*, 41-50. https://doi.org/10.1016/j.jcis.2008.03.013.
Veiga-Santos, P., Suzuki, C. K., Cereda, M. P., & Scamparini, A. R. P. (2005). Microstructure and color of starch–gum films: Effect of gum deacetylation and additives. Part 2. *Food Hydrocolloids, 19*(6), 1064-1073. https://doi.org/10.1016/j.foodhyd.2005.02.007.
Verma, D. K., Niamah, A. K., Patel, A. R., Thakur, M., Sandhu, K. S., Chavez-Gonzalez, M. L., Shah, N., & Noe Aguilar, C. (2020). Chemistry and microbial sources of curdlan with potential application and

safety regulations as prebiotic in food and health. *Food Research International, 133*, 109136. https://doi.org/10.1016/j.foodres.2020.109136.

Villanueva, M., De Lamo, B., Harasym, J., & Ronda, F. (2018). Microwave radiation and protein addition modulate hydration, pasting and gel rheological characteristics of rice and potato starches. *Carbohydrate Polymers, 201*, 374-381. https://doi.org/10.1016/j.carbpol.2018.08.052.

Wang, S., Ren, J., Li, W., Sun, R., & Liu, S. (2014). Properties of polyvinyl alcohol/xylan composite films with citric acid. *Carbohydrate Polymers, 103*, 94-99. http://dx.doi.org/10.1016/j.carbpol.2013.12.030.

Wang, Y., Yu, L., Xie, F., Li, S., Sun, Q., Liu, H., & Chen, L. (2018). On the investigation of thermal/cooling-gel biphasic systems based on hydroxypropyl methylcellulose and hydroxypropyl starch. *Industrial Crops and Products, 124*, 418-428. https://doi.org/10.1016/j.indcrop.2018.08.010.

Xiao, M., Jiang, M., Wu, K., Yang, H., Ni, X., Yan, W., Phillips, G. O., & Jiang, F. (2017). Investigation on curdlan dissociation by heating in water. *Food Hydrocolloids, 70*, 57-64. http://dx.doi.org/10.1016/j.foodhyd.2017.03.018.

Yuan, C., Xu, D., Cui, B., & Wang, Y. (2019). Gelation of κ-carrageenan/Konjac glucommanan compound gel: Effect of cyclodextrins. *Food Hydrocolloids, 87*, 158-164. https://doi.org/10.1016/j.foodhyd.2018.07.037.

Zhang, M., Jia, R., Ma, M., Sun, Q., Li, M., & Xie, F. (2024). Effect of sheeting stress and heating on the molecular chain structure, size, and conformation of gluten proteins during noodle processing. *Food Hydrocolloids, 146*, 109266. https://doi.org/10.1016/j.foodhyd.2023.109266.

Zhou, L., Fu, J., Bian, L., Chang, T., & Zhang, C. (2022). Preparation of a novel curdlan/bacterial cellulose/cinnamon essential oil blending film for food packaging application. *International Journal of Biological Macromolecules, 212*, 211-219. https://doi.org/10.1016/j.ijbiomac.2022.05.137.

Figure Captions

Fig. 1. G', G'' and tan δ curves for RS-CD composite gels (10:0, 7:3, 5:5, 3:7, and 0:10) in temperature scanning mode

Fig. 2. SAXS intensity profiles (a) and ln$I$ *vs.* ln$q$ curves with their fitted lines (b) for RS-CD composite gels (10:0, 7:3, 5:5, 3:7, and 0:10).

Fig. 3. SEM images of RS-CD composite gels (10:0, 7:3, 5:5, 3:7, and 0:10) at 500 × and 1000 ×.

Fig. 4. FTIR spectra of RS-CD composite gels (10:0, 7:3, 5:5, 3:7, and 0:10).

Fig. 5. Textural properties of RS-CD composite gels (10:0, 7:3, 5:5, 3:7, and 0:10) at 25 °C and 85 °C. Within one group (either a, b, c, d, and e, or A, B, C, D and E), different letters mean significant difference at 25 °C and 85 °C ($p < 0.05$).

Fig. 6. Schematic representation of temperature-induced structural changes of pure RS, CD and RS-CD composites.

- Supplementary material -

On the investigation of composite cooling/heating set gel systems based on rice starch and curdlan

Jing Wang[1], Qianhui Ma[1], Pingxiong Cai[2], Xinyu Sun[1], Qingjie Sun[1,3], Man Li[1,3,*], Yanfei Wang[1,3,†], Lei, Zhong[4], Fengwei Xie[5]

[1]*College of Food Science and Engineering, Qingdao Agricultural University, Qingdao, Shandong 266109, China*

[2]*Guangxi Key Laboratory of Green Chemical Materials and Safety Technology, Guangxi Engineering Research Center for New Chemical Materials and Safety Technology, Beibu Gulf University, Qinzhou, Guangxi 535000, China*

[3]*Qingdao Special Food Research Institute, Qingdao, Shandong 266109, China*

[4]*Guangxi Key Laboratory for Polysaccharide Materials and Modifications, Guangxi Higher Education Institutes Key Laboratory for New Chemical and Biological Transformation Process Technology, School of Chemistry and Chemical Engineering, Guangxi Minzu University, Nanning, Guangxi 530006, China*

[5]*School of Engineering, Newcastle University, Newcastle upon Tyne, NE1 7RU, United Kingdom*

[*]Corresponding author. *E-mail address*: manliqau@163.com (M. Li),

[†]Corresponding author. *E-mail addresses*: yanfeiwang@qau.edu.cn; yanfeiwangqau@163.com (Y. Wang)

List of supplementary figures

List of supplementary tables

FIGURTES

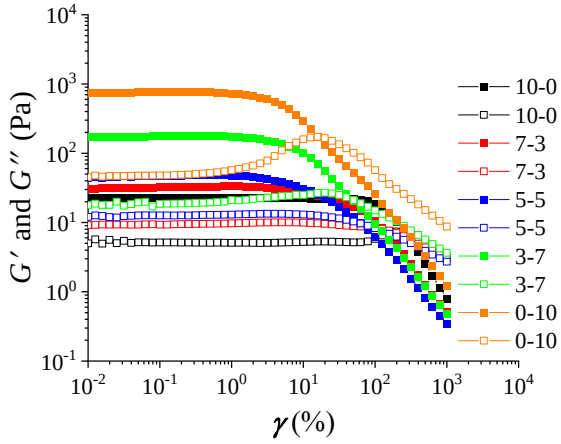

Fig. S1. Strain-sweep curves for RS-CD composite gels (10:0, 7:3, 5:5, 3:7, and 0:10) at a frequency of 1Hz at 25 °C.

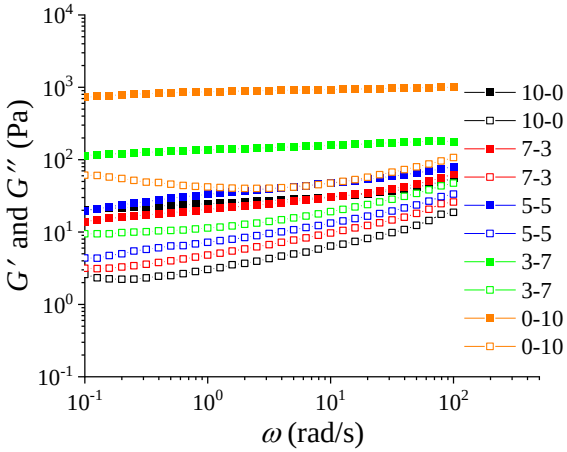

Fig. S2. G′ (solid) and G″ (open) curves for RS-CD composite gels (10:0, 7:3, 5:5, 3:7, and 0:10) in frequency scanning mode at 25 °C.

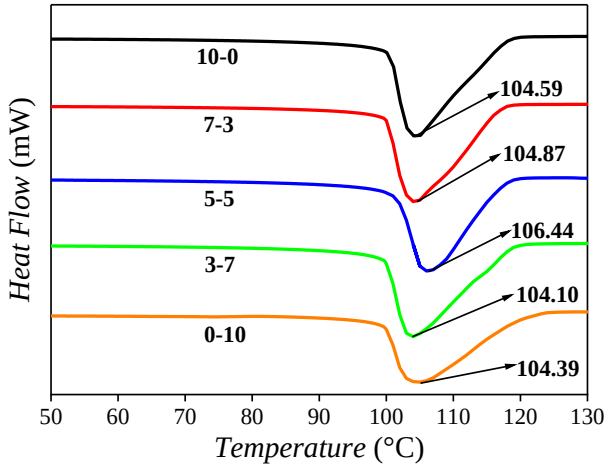

Fig. S3. DSC curves for RS-CD composite gels (10:0, 7:3, 5:5, 3:7, and 0:10).

TABLES

Table S1. n', n'', G_0', and G_0'' for RS-CD composite gels (10:0, 7:3, 5:5, 3:7, and 0:10) at 25 °C as determined from Eqs. (1) and (2).

RS/CD	n'	G_0' (Pa)	R^2	n''	G_0'' (Pa)	R^2
10:0	0.164±0.006[a]	23.423±0.933[a]	0.8951±0.026	0.3852±0.003[a]	2.721±0.066[a]	0.9821±0.004
7:3	0.155±0.002[b]	26.144±0.305[b]	0.9724±0.011	0.3508±0.003[b]	4.940±0.028[b]	0.9879±0.001
5:5	0.132±0.009[c]	39.363±0.733[c]	0.9542±0.008	0.3258±0.000[c]	5.351±0.345[c]	0.9856±0.003
3:7	0.072±0.010[d]	135.787±0.590[d]	0.9813±0.024	0.3126±0.008[d]	9.895±0.311[d]	0.9747±0.003
0:10	0.034±0.003[e]	851.397±17.931[e]	0.9890±0.013	0.2141±0.006[e]	32.524±0.841[e]	0.8789±0.016

Note: Data are rendered as mean ± standard deviation. Different letters (a, b, c, d, and e) mean significant difference ($p < 0.05$).

Table S2. Moisture content of RS-CD composite gels (10:0, 7:3, 5:5, 3:7, and 0:10) for SAXS measurement.

RS/CD	Moisture content (%)
10:0	91.92±1.44
7:3	92.26±0.93
5:5	92.15±0.92
3:7	91.79±0.73
0:10	92.23±0.49

Table S3. *G′* values of RS-CD composite gels (10:0, 7:3, 5:5, and 3:7) at 30 °C and 90 °C, respectively.

G′(Pa)	30 °C	90 °C
10:0	24.58±1.31[a]	9.44±0.27[a]
7:3	28.74±0.18[b]	17.01±1.14[b]
5:5	32.94±1.22[c]	33.25±3.97[c]
3:7	129.88±8.50[d]	106.70±2.09[d]

Note: Data are rendered as mean ± standard deviation. Different letters (a, b, c, and d) mean significant difference ($p < 0.05$).

Table S4. Fractal structure parameters of RS-CD composite gels (10:0, 7:3, 5:5, 3:7, and 0:10).

RS/CD	α	D
10:0	2.25±0.02[a]	2.25±0.02 [a]
7:3	2.33±0.02[b]	2.33±0.02 [b]
5:5	2.34±0.02[b]	2.34±0.02 [b]
3:7	2.39±0.02[c]	2.39±0.02 [c]
0:10	2.41±0.01[c]	2.41±0.01 [c]

Note: Data are rendered as mean ± standard deviation. Different letters (a, b, and c) mean significant difference ($p < 0.05$).

Table S5. Enthalpy values of RS-CD composite gels (10:0, 7:3, 5:5, 3:7, and 0:10).

RS/CD	Enthalpy (J/g)
10:0	14623.00±398.04[a]
7:3	15010.00±580.00[a]
5:5	16490.00±478.43[b]
3:7	16703.33±195.02[b]
0:10	17185.00±190.92[b]

Note: Data are rendered as mean ± standard deviation. Different letters (a and b) mean significant difference ($p < 0.05$).